MATHEMATICS OF COMPUTATION
Volume 84, Number 292, March 2015, Pages 563–579
S 0025-5718(2014)02871-8
Article electronically published on August 14, 2014

THE MINIMAL CONFORMING H^k FINITE ELEMENT SPACES ON R^n RECTANGULAR GRIDS

JUN HU AND SHANGYOU ZHANG

ABSTRACT. A family of C^{k-1}-Q_k finite elements on R^n rectangular grids is constructed. The finite element space is shown to be the full C^{k-1}-Q_k space and possess the optimal order of approximation property. The polynomial degree is minimal in order to form such a H^k finite element space. Numerical tests are provided for using the 2D C^1-Q_2 and C^2-Q_3 finite elements.

1. Introduction

Recently, Wang and Xu proposed a family of nonconforming finite elements for $2k$-th order (any k) elliptic partial differential equations in R^n, on triangular grids [21]. The polynomial degree of finite element is k for $2k$-th order PDEs in R^n for any $n \geq k$. This is extremely simple when compared to the standard conforming elements. For example, for $m = 2, 3, 4$ and $n = 3$, the polynomial degrees of the 3D C^1, C^2 and C^3 spaces are 9, 17 and 25, respectively (cf. [2,4,24]), while those of the Wang-Xu elements are 2, 3 and 4 only, respectively. What is the minimal polynomial degree on rectangular grids, for conforming and nonconforming finite elements? We will answer the first question in this paper.

The polynomial degree of the minimal H^k-conforming element, i.e, the C^{k-1}-Q_m finite element, in any dimensional space R^n is simply $m = k$. Here Q_k is the space of polynomials of separated degree k or less. We note that C^{k-1} is the minimal smoothing space for $2k$-th-order PDE, i.e., $C^{k-1} \subset H^k$, so-called H^k-conforming. We construct the C^{k-1}-Q_k space through the tensor products of 1D splines [18], as shown in Figure 1. The spaces constructed are macro-element spaces, as in [17]. We show that the tensor product space is the full C^{k-1}-Q_k space on rectangular grids, i.e., all C^{k-1}-Q_k functions must belong to the tensor product space. On the other side, any $(k-1)$-st derivatives of a degree k polynomial is a linear function in n-dimensional space, which is of the minimal degree to have a global continuity. If we decrease the polynomial degree further, then we get a global polynomial space, i.e., the C^{k-1}-Q_{k-1} space is the global Q_{k-1} space. Thus we say the C^{k-1}-Q_k space is the minimal Q_m space to be C^{k-1}, i.e, the minimal H^k-conforming finite element. This work extends the C^1-Q_2 result in [10]. When compared to the Wang-Xu element, ours is slightly bigger, Q_k versus P_k, though both are said to be degree-k polynomials. But the new C^{k-1}-Q_k conforming space exists for any

Received by the editor January 27, 2013 and, in revised form, May 10, 2013, June 6, 2013, and August 1, 2013.

2010 *Mathematics Subject Classification.* Primary 65N30.

Key words and phrases. Conforming finite element, rectangular grid.

The first author was supported by the NSFC Project 11271035, and in part by the NSFC Key Project 11031006.

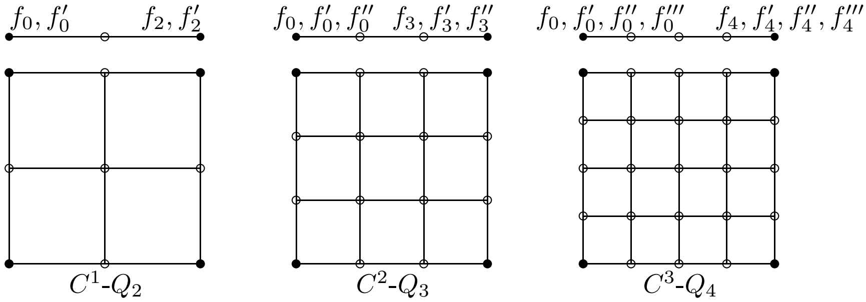

FIGURE 1. Tensor products of 1D C^1-Q_1, C^2-Q_3 and C^3-Q_4 in 2D.

spacial dimension n, while the Wang-Xu nonconforming spaces limit $n \geq k$; cf. [21]. We note that the standard C^{k-1}-Q_m finite element requires the polynomial degree $m \geq 2k-1$, i.e., C^1-Q_3, C^2-Q_5 and so on; cf. [25]. Here the new elements are C^1-Q_2, C^2-Q_3 and so on. Numerical tests on these elements for biharmonic and triharmonic equations are provided.

The second question about the minimal nonconforming H^k elements on rectangular grids remains open for $k > 1$. For $k = 1$, the minimal H^1-nonconforming element is the C^{-1}-P_1 element (where the P_1 functions are continuous at the mid-point of the $(n-1)$-rectangular face) on rectangular grids [11, 16]. An H^2-nonconforming element on rectangular grids, is constructed by Wang, Shi and Xu [22], in R^n. But it is not clear if the Wang-Shi-Xu element is the minimal one. Such a question is difficult to answer for nonconforming finite elements as there are too many possible variations. For example, it is not even known what the minimal H^1-nonconforming P_2 element is on rectangular grids. In [15] Lee and Sheen constructed such a nonconforming element where P_2 space is enriched by two bubbles $\{x^2y, xy^2\}$. Note that a direct corollary of [9, Section 5.1] is that there does not exist a conforming P_2 element on rectangular grids (even macro-element), otherwise the term of (5.12) therein will have convergence of order 3, which contracts with the lower bound of (5.12) therein.

In 1D, our C^{k-1}-Q_k nodal basis generates exactly the k-th B-spline space, if the macro-element grid points are uniformly distributed. The B-spline space has only one basis function, defined recursively by integration, which is shifted by the grid size to form a smooth spline space; cf. (2.6) below. Using the tensor product of B-splines, the method of *spline finite element method* is applied to solving partial differential equations in [20]. Different from the spline finite element method, we construct nodal basis functions which are more adaptive to boundary conditions and to the traditional finite element computation. The other difference is that the C^{k-1}-Q_k nodal basis can be constructed on nonuniform local grids, and applied to nonuniform global grids. One numerical test on nonuniform grids is provided.

2. TENSOR PRODUCT SPACE

We define a family of 1D spline functions. Using the 1D splines, we define a C^{k-1}-Q_k space in any space dimension, by tensor product.

Let $[0,1]$ be uniformly partitioned into k intervals by $(k+1)$ points $\{x_i = i/k,\ i = 0,1,\ldots,k\}$:

$$\mathcal{T}_h^{(1)} = \{[x_{i-1}, x_i] \ \mid \ i = 1,\ldots,k\}. \tag{2.1}$$

Here, the internal grid points $\{x_i\}$ are not necessarily uniformly distributed; cf. Corollary 2.1. Let

$$P_k(\mathcal{T}_h^{(1)}) = \{f \in L^2([0,1]) \mid f|_{(x_{i-1},x_i)} \in P_k\}$$

be the space of piecewise polynomials of degree-k. Let I_0 be an interpolation operator (cf. Figure 1),

$$\begin{aligned} &I_0 : C^{k-1}[0,1] \to V_0 := P_k(\mathcal{T}_h^{(1)}) \cap C^{k-1}[0,1], \qquad (2.2)\\ &I_0 f^{(i)}(x_0) = f^{(i)}(x_0), \quad I_0 f^{(i)}(x_k) = f^{(i)}(x_k), \quad i = 0,1,\ldots,k-1. \end{aligned}$$

Here $h = 1/k$ is called a grid size.

Theorem 2.1. *I_0 in (2.2) is well defined.*

Proof. Let us count the dof (degrees of freedom) and the constraints. The dof of one P_k polynomial is $(k+1)$. The total dof on k intervals is (k^2+k). To be C^{k-1} at the two end points x_0 and x_k, we have $(2k)$ data. But at each of the $(k-1)$ middle points, to be C^{k-1}, we have k constraints. The total constraints are $(2k) + (k-1)k = k^2 + k$, matching the total dof. By these counts, we have a square linear system of size (k^2+k). Therefore, the uniqueness implies existence. We are now left to show the uniqueness of solution.

Let $f \in V_0$ in (2.2). First, as $f(x_0) = 0, f'(x_0) = 0, \ldots, f^{(k-1)}(x_0) = 0$, by Taylor expansion at $x = x_0$, we have, on $[x_0, x_1)$,

$$f(x) = c_1(x - x_0)^k \quad \text{ on } [x_0, x_1).$$

We expand the function at $x = x_1$ to get

$$\begin{aligned} (x-x_0)^k &= (x - x_1 + h)^k \\ &= h^k + kh^{k-1}(x-x_1) + \cdots + kh(x-x_1)^{k-1} + (x-x_1)^k. \end{aligned}$$

By the continuity conditions on $f^{(j)}(x_1)$, we can expand the function, also a polynomial, on the second interval, (x_1, x_2),

$$\begin{aligned} f(x) &= c_1(h^k + kh^{k-1}(x-x_1) + \cdots + kh(x-x_1)^{k-1}) + c_2'(x-x_1)^k \\ &= c_1(x-x_0)^k + c_2(x-x_1)^k. \end{aligned}$$

Sequentially, we derive the function on the last interval (x_{k-1}, x_k):

$$f(x) = c_1(x-x_0)^k + \cdots + c_k(x-x_{k-1})^k.$$

As $f^{(j)}(x_k) = 0$, $x_k - x_i = (k-i)h$,

$$k(k-1)\cdots(k-j+1)(c_1 k^{k-j} + \cdots + c_k 1^{k-j})h^{k-j} = 0.$$

So, $\{c_j\}$ are determined by the homogeneous system:

$$\begin{pmatrix} k^k & \cdots & 2^k & 1^k \\ k^{k-1} & \cdots & 2^{k-1} & 1^{k-1} \\ \vdots & & & \\ k & \cdots & 2 & 1 \end{pmatrix} \begin{pmatrix} c_1 \\ c_2 \\ \vdots \\ c_k \end{pmatrix} = 0.$$

The matrix is a Vandermonde matrix, and its determinant is nonzero,

$$\det = (k!) \cdots (2!) \cdot (1!).$$

Thus, I_0 is uniquely defined. $\square$

Corollary 2.1. *I_0 in* (2.2) *is well defined for any nonuniform grid in* (2.1)*:*

$$0 = x_0 < x_1 < \cdots < x_k = 1.$$

Proof. The proof repeats that of Theorem 2.1 except replacing the uniform grid size h, there, by

$$h_i = x_i - x_{i-1}.$$

Then the linear system determining $f(x)$ is

$$\begin{pmatrix} (\sum_{i=1}^k h_i)^k & \cdots & (\sum_{i=k-1}^k h_i)^k & h_k^k \\ (\sum_{i=1}^k h_i)^{k-1} & \cdots & (\sum_{i=k-1}^k h_i)^{k-1} & h_k^{k-1} \\ \vdots & & & \\ \sum_{i=1}^k h_i & \cdots & \sum_{i=k-1}^k h_i & h_k \end{pmatrix} \begin{pmatrix} c_1 \\ \vdots \\ c_{k-1} \\ c_k \end{pmatrix} = 0.$$

The coefficient matrix is again a Vandermonde matrix, and its determinant is nonzero. $\square$

Given k sets of linearly independent nodal values $f^{(i)}(0)$, $f^{(i)}(1)$, $i = 0, 1, \ldots, k-1$, the interpolation operator I_0 defines a set of basis functions. That is, a basis $\{\phi_{i_0,j_0}\}$ is defined such that

$$\frac{d^{i_1}}{dx^{i_1}} \phi_{i_0,j_0}(j_1) = \delta_{i_1,i_0}\delta_{j_1,j_0}, \quad 0 \le i_1, i_0 \le (k-1),\ j_1, j_0 = 0, 1. \tag{2.3}$$

For example, the 6 nodal basis functions for the C^2-P_3 space V_0 on $[0,1]$ are

$$\phi_{0,0} = \begin{cases} 1 - \frac{9}{2}x^3, & 0 \le x < \frac{1}{3}, \\ \frac{1}{2} + \frac{9}{2}x - \frac{27}{2}x^2 + 9x^3, & \frac{1}{3} \le x < \frac{2}{3}, \\ -\frac{9}{2}(x-1)^3, & \frac{2}{3} \le x \le 1, \qquad \phi_{0,0}(0) = 1, \end{cases} \tag{2.4}$$

$$\phi_{1,0} = \begin{cases} -x(-1 + 3x^2), & 0 \le x < \frac{1}{3}, \\ -\frac{5}{18} + \frac{7}{2}x - \frac{15}{2}x^2 + \frac{9}{2}x^3, & \frac{1}{3} \le x < \frac{2}{3}, \\ -\frac{3}{2}(x-1)^3, & \frac{2}{3} \le x \le 1, \quad \phi_{1,0}'(0) = 1, \end{cases}$$

$$\phi_{2,0} = \begin{cases} -\frac{1}{12}x^2(-6 + 11x), & 0 \le x < \frac{1}{3}, \\ -\frac{1}{18} + \frac{1}{2}x - x^2 + \frac{7}{12}x^3, & \frac{1}{3} \le x < \frac{2}{3}, \\ -\frac{1}{6}(x-1)^3, & \frac{2}{3} \le x \le 1, \quad \phi_{2,0}''(0) = 1, \end{cases}$$

$$\phi_{0,1} = \begin{cases} \frac{9}{2}x^3, & 0 \le x < \frac{1}{3}, \\ \frac{1}{2} - \frac{9}{2}x + \frac{27}{2}x^2 - 9x^3, & \frac{1}{3} \le x < \frac{2}{3}, \\ 1 + \frac{9}{2}(x-1)^3, & \frac{2}{3} \le x \le 1, \qquad \phi_{0,1}(1) = 1, \end{cases}$$

$$\phi_{1,1} = \begin{cases} -\frac{3}{2}x^3, & 0 \le x < \frac{1}{3}, \\ -\frac{2}{9} + 2x - 6x^2 + \frac{9}{2}x^3, & \frac{1}{3} \le x < \frac{2}{3}, \\ -(x-1)(2-6x+3x^2), & \frac{2}{3} \le x \le 1, \quad \phi'_{1,1}(1) = 1, \end{cases}$$

$$\phi_{21} = \begin{cases} \frac{1}{6}x^3, & 0 \le x < \frac{1}{3}, \\ \frac{1}{36} - \frac{1}{4}x + \frac{3}{4}x^2 - \frac{7}{12}x^3, & \frac{1}{3} \le x < \frac{2}{3}, \\ \frac{1}{12}(x-1)^2(11x-5), & \frac{2}{3} \le x \le 1, \quad \phi''_{2,1}(1) = 1. \end{cases}$$

The global basis functions in 1D combines above two local basis functions on the left and on the right intervals of a node:

$$\varphi_i(x) = \begin{cases} \phi_{i,1}(x+1) & -1 \le x \le 0, \\ \phi_{i,0}(x-0) & 0 < x \le 1, \end{cases} \qquad i = 0, 1, \ldots, k-1. \tag{2.5}$$

We note that, for uniform grids, the 1D C^{k-1}-P_k finite element space is exactly the k-th B-spline space, [18, 20]. So we give another proof of the existence of B-splines in Theorem 2.1. We give the P_3 B-spline basis below to show that our C^2-P_3 basis functions above are truly linear combinations of this (shifted-scaled) B-spline basis. Let

$$B_0(x) = \begin{cases} 0 & x < -1/2, \\ 1 & -1/2 \le x < 1/2, \\ 0 & 1/2 \le x. \end{cases}$$

The k-th B-spline is defined by

$$B_k(x) = \frac{1}{k}(\frac{k+1}{2} + x)B_{k-1}(x + \frac{1}{2}) + \frac{1}{k}(\frac{k+1}{2} - x)B_{k-1}(x - \frac{1}{2}).$$

Sequentially, we get that

$$B_1(x) = \begin{cases} 0 & x < -1, \\ 1 + x & -1 \le x < 0, \\ 1 - x & 0 \le x < 1, \\ 0 & 1 \le x, \end{cases}$$

$$B_2(x) = \begin{cases} 0 & x < -3/2, \\ \frac{1}{2}(\frac{3}{2}+x)^2 & -3/2 \le x < -1/2, \\ \frac{1}{2}(\frac{3}{2}+x)(\frac{1}{2}-x) + \frac{1}{2}(\frac{3}{2}-x)(\frac{1}{2}+x) & -1/2 \le x < 1/2, \\ \frac{1}{2}(\frac{3}{2}-x)^2 & 1/2 \le x < 3/2, \\ 0 & 3/2 \le x, \end{cases}$$

$$B_3(x) = \begin{cases} 0 & x < -2, \\ \frac{1}{6}(2+x)^3 & -2 \le x < -1, \\ \frac{2}{3} - x^2 - \frac{1}{2}x^3 & -1 \le x < 0, \\ \frac{2}{3} - x^2 + \frac{1}{2}x^3 & 0 \le x < 1, \\ \frac{1}{6}(2-x)^3 & 1 \le x < 2, \\ 0 & 2 \le x. \end{cases} \tag{2.6}$$

We can then combine some B_3 functions to get the 6 basis functions above. For example, the basis function in (2.4) is also

$$\phi_{0,0}(x) = B_3(3x-1) + B_3(3x) + B_3(3x+1), \quad x \in (0, 1/3).$$

One may use nonnodal basis functions like (2.6) directly in solving partial differential equations. Such a method is called the method of *spline finite element* [20].

Let a square (or a rectangular) domain $\Omega \subset R^n$ be partitioned into $(kN)^n$ n-rectangles:

$$\mathcal{T}_h = \{[x^{(1)}_{i_1,j_1-1}, x^{(1)}_{i_1,j_1}] \times \cdots \times [x^{(n)}_{i_n,j_n-1}, x^{(n)}_{i_n,j_n}] \mid 1 \le i_l \le N, \\ 1 \le j_l \le k, \ 1 \le l \le n\}. \tag{2.7}$$

Here, for simplicity, we assume a uniform grid of macro-elements:

$$x^{(n_l)}_{i_l+1,0} - x^{(n_l)}_{i_l,0} = h = \frac{1}{N}, \quad x^{(n_l)}_{i_l,j_l+1} - x^{(n_l)}_{i_l,j_l} = \frac{1}{kN}.$$

But we can allow variable grid points inside a macro-element (consisting of k^n n-dimensional rectangles), or variable macro-element sizes, such as one in our numerical test, shown in Figure 6. We define a piecewise Q_k finite element space by

$$V_h = \{ \sum_{i_1,\ldots i_n=0}^{N} \sum_{j_1,\ldots,j_n=0}^{k-1} c^{i_1,\ldots,i_n}_{j_1,\cdots,j_n} \varphi^{i_1,\ldots,i_n}_{j_1,\cdots,j_n}(x_1,\ldots,x_n)\}. \tag{2.8}$$

Here $\varphi^{i_1,\ldots,i_n}_{j_1,\cdots,j_n}$ is the shifted, scaled tensor product basis function:

$$\varphi^{i_1,\ldots,i_n}_{j_1,\cdots,j_n}(x_1,\ldots,x_n) = h^{j_1}\varphi_{j_1}(\frac{x_1 - x^{(1)}_{i_1}}{h}) \cdots h^{j_n}\varphi_{j_n}(\frac{x_n - x^{(n)}_{i_n}}{h}). \tag{2.9}$$

Here $x^{(1)}_{i_1} = x^{(1)}_{i_1,0}$ is an end point of macro-element

Outside the domain Ω, we naturally drop the part of definition of $\varphi_{j_1,\cdots,j_n}$.

3. The full C^{k-1}-Q_k space

We will show that the finite element space V_h defined in (2.8) is truly a C^{k-1} space. We define an interpolation operator from C^{k-1} to V_h. By this operator, we will show the space (2.8) is the whole C^{k-1}-Q_k on the grid.

Given the n-dimensional rectangular grid $\mathcal{T}_h$ in (2.7), the mathematical (abstract) definition of C^{k-1}-Q_k is

$$\tilde{V}_h = \{v \in C^{k-1}(\Omega) \mid v|_K \in Q^n_k \quad \forall K \in \mathcal{T}_h\}, \tag{3.1}$$

where Q^n_k is the n-dimensional Q_k space. Is $\tilde{V}_h = V_h$ (defined in (2.8))? If we show $V_h \subset C^{k-1}(\Omega)$, then $\tilde{V}_h \supset V_h$, as the latter is the full space. On the other side, if the interpolation of a $\tilde{V}_h$ function in V_h is itself, then $\tilde{V}_h \subset V_h$.

We define the nodal interpolation operator

$$I_h \; : \; C^{k-1}(\Omega) \to V_h, \qquad v \mapsto I_h v, \tag{3.2}$$

$$I_h v = \sum_{i_1,\dots i_n=0}^{N} \sum_{j_1,\dots,j_n=0}^{k-1} c_{j_1,\cdots,j_n}^{i_1,\dots,i_n} \varphi_{j_1,\cdots,j_n}^{i_1,\dots,i_n}(x_1,\dots,x_n), \tag{3.3}$$

where the coefficients are nodal values:

$$c_{j_1,\cdots,j_n}^{i_1,\dots,i_n} = \frac{\partial^{j_1}}{\partial x_1^{j_1}} \cdots \frac{\partial^{j_n}}{\partial x_n^{j_n}} v(x_{i_1}^{(1)},\dots,x_{i_n}^{(n)}).$$

Theorem 3.1. *The space V_h defined in* (2.8) *is a C^{k-1} space.*

Proof. Usually, C^{k-1} means the continuity of all derivatives up to the total order $(k-1)$, or to the separated order $(k-1)$, i.e.,

$$\frac{\partial^{j_1}}{\partial x_1^{j_1}} \cdots \frac{\partial^{j_n}}{\partial x_n^{j_n}} v \qquad \text{for } 0 \le j_1 + \cdots + j_n \le k-1, \qquad \text{or } 0 \le j_1,\dots,j_n \le k-1.$$

Here we take the latter definition which is stronger. For any $v \in V_h$, it is a linear combination of the basis functions. We only need to check if all basis functions are C^{k-1}. All the 1D basis $\phi_{i,j}$ in (2.3) and the φ_i in (2.5) have all their derivatives up to order $k-1$ matching on the two sides of each grid point, i.e. $\varphi_i^{(j)}$ is continuous. So, the shifted scaled product is also continuous by (2.9),

$$\begin{aligned} &\frac{\partial^{j_1}}{\partial x_1^{j_1}} \cdots \frac{\partial^{j_n}}{\partial x_n^{j_n}} \varphi_{j'_1,\cdots,j'_n}^{i'_1,\dots,i'_n} \\ &= \frac{h^{j_1}}{h^{j'_1}} \frac{\partial^{j_1}}{\partial x_1^{j_1}} \varphi_{j'_1}\Big(\frac{x_1 - x_{i'_1}^{(1)}}{h}\Big) \cdots \frac{h^{j_n}}{h^{j'_n}} \frac{\partial^{j_n}}{\partial x_n^{j_n}} \varphi_{j'_n}\Big(\frac{x_n - x_{i'_n}^{(n)}}{h}\Big), \end{aligned}$$

as it is a product of continuous functions (each remains constant in the other $n-1$ directions). Thus $\varphi_{j_1,\cdots,j_n}^{i_1,\dots,i_n} \in C^{k-1}$. So $v \in C^{k-1}$. ☐

Theorem 3.2. *The space V_h defined in* (2.8) *is the full C^{k-1}-Q_k space, i.e., $V_h = \tilde{V}_h$, defined in* (3.1).

Proof. By Theorem 3.1, $V_h \subset \tilde{V}_h$. To prove the reverse, we show that $I_h v = v \in V_h$ for every $v \in \tilde{V}_h$.

To illustrate the method, we first consider the case $n = 2$, $k = 3$ and $N = 1$, shown in Figure 2. By the data of v, $I_h v$ is well defined. As $v \in C^2([0,1]^2)$, its restriction on line BD (see Figure 2) is a 1D C^2-P_3 function. By Theorem 2.1, $v \equiv I_h v$ on line BD. Next, when $\partial(v - I_h v)/\partial y$ restricted on line BD, calling it w_y, it is still a C^2-P_3 function in x. As $\partial^j w_y(0) = \partial^j w_y(1) = 0$, $j = 0,1,2$, by Theorem 2.1, $w_y \equiv 0$. Once again, $w_{yy} = \partial^2(v - I_h v)/\partial y^2|_{BD} \equiv 0$. Thus, all 9 interpolation data of $v - I_h v$ are 0 at an internal point C of BD. In the same fashion, $v - I_h v$ has all 9 interpolation data 0 at point A; cf. Figure 2. Repeating the argument on AC, we find $v - I_h v$ has all 9 interpolation data 0 at point F. We conclude $v \equiv I_h v$ on square $CDEF$, as all their 36 interpolation values at four corners are identical (while they have 4×4 dof). Hence $v = I_h v$.

We now formally show, for all $v \in \tilde{V}_h$,

$$I_h v = v, \tag{3.4}$$

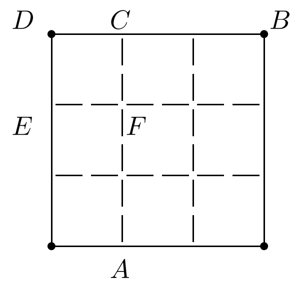

FIGURE 2. Interpolating a C^2-Q_3 function v on one macro-element, in 2D.

by a space-dimension reduction method. We examine the difference $u = I_h v - v$ on any macro-element $K = [x^{(1)}_{i_1,0}, x^{(1)}_{i_1,k}] \times \cdots \times [x^{(n)}_{i_n,0}, x^{(n)}_{i_n,k}]$ which consists of k^n small squares. When restricted on one boundary edge of K,

$$[x^{(1)}_{i_1,0}, x^{(1)}_{i_1,k}] \times \{x^{(2)}_{i_2,j_2}\} \times \cdots \times \{x^{(n)}_{i_n,j_n}\}$$

where $j_2, \cdots, j_n = 0$ or k, $I_h v$ depends only on the data of v at the two end points of the edge, as all other basis functions vanish at the edge. $I_h v$ and v are both 1D C^{k-1}-P_k functions on the k intervals of the edge of K. By Theorem 2.1, $I_h v$ is the unique interpolation $I_0 v$ of v, defined in (2.2), i.e., $I_h v - v = 0$ on the edge. Repeating the above argument for any partial derivatives (normal to the edge) of order smaller than k, when restricted on the edge, we get

$$\frac{\partial^{j_2}}{\partial x_1^{j_2}} \cdots \frac{\partial^{j_n}}{\partial x_n^{j_n}} (I_h v - v)(x_1, x^{(2)}_{i_2,0}, \ldots, x^{(n)}_{i_n,0}) \equiv 0, \quad x_1 \in [x^{(1)}_{i_1,0}, x^{(1)}_{i_1,k}]$$

for all $0 \le j_2, \cdots, j_n \le k-1$. Now, restricted on a face-internal edge,

$$\{x^{(1)}_{i_1,l_1}\} \times [x^{(2)}_{i_2,0}, x^{(2)}_{i_2,k}] \times \{x^{(3)}_{i_3,j_3}\} \times \cdots \times \{x^{(n)}_{i_n,j_n}\}, \quad 0 < l_1 < k,$$

on a face square of K,

$$[x^{(1)}_{i_1,0}, x^{(1)}_{i_1,k}] \times [x^{(2)}_{i_2,0}, x^{(2)}_{i_2,k}] \times \{x^{(3)}_{i_3,j_3}\} \times \cdots \times \{x^{(n)}_{i_n,j_n}\}$$

where $j_3, \cdots, j_n = 0$ or k, we have the two end points on the boundary edges considered above. So $I_h v$ matches v with all end point data, proved above, and $I_h v = v$ on such an internal edges. Repeating this argument for the two functions and their derivatives, we see that $I_h v$, v and all their derivatives match at all $(k+1)^n$ edges. Now, on each square of K we get

$$[x^{(1)}_{i_1,0}, x^{(1)}_{i_1,k}] \times [x^{(2)}_{i_2,0}, x^{(2)}_{i_2,k}] \times \{x^{(3)}_{i_3,j_3}\} \cdots \times \{x^{(n)}_{i_n,j_n}\}$$

where $j_3, \cdots, j_n = 0$ or k, $u \in Q_k^2$ but with its value all up to $k-1$ (normal, tangential, or mixed) order derivatives of 0. So $u \equiv 0$ on the square. Then we work on 3D face-cubes of K, and so on, until its n-dimensional face, which is itself. Thus $u = 0$ on K and on Ω. Therefore $v = I_h v \in V_h$, i.e., $\tilde{V}_h \subset V_h$. $\square$

4. THE FULL ORDER OF APPROXIMATION

By the interpolation operator I_h, we will show the C^{k-1}-Q_k space has the full order of approximation property. Finally, we use the element for solving $2k$-th order Laplace equations and show its optimal order of convergence.

In (3.2), interpolation I_h uses the cross derivative of order $(k-1)^n$:

$$\frac{\partial^{k-1}}{\partial x_1^{k-1}} \cdots \frac{\partial^{k-1}}{\partial x_n^{k-1}} f(x_{i_1}^{(1)}, \ldots, x_{i_n}^{(n)}).$$

By the Sobolev inequality [5], the function has to be in $C^{(k-1)n}(\Omega)$ or

$$f \in H^{(k-1)n+n/2+\epsilon}(\Omega). \tag{4.1}$$

For example, for the 3D C^3-Q_4 space, the function f to be interpolated must be in $H^{13.5+\epsilon}$. Since the smoothness is too high, we cannot develop the needed approximation for weak solutions of $2k$-th order PDE. That is, for the 3D C^3-Q_4 space, the function u to be interpolated is assumed only in H^4. Therefore, a generalization of I_h, i.e, averaging I_h is needed (still denoted as I_h). It was first done by Scott and Zhang [19], for Lagrange finite elements, and it was generalized to Hermite elements by Girault and Scott [8]. We extended the Girault-Scott operator to high-order derivative (more than 2) interpolation. That is, the $(k-1)^n$ nodal derivatives are defined by averaging the boundary data on a R^{n-1} face square of H^k weak functions.

For each set of cross-derivatives $D_{(\alpha_2,\cdots,\alpha_n)} = \{\partial^\alpha f \mid 0 \le \alpha_1 \le k-1\}$, we need a set of dual basis of C^{k-1}-Q_k polynomials. First we consider the nodal interpolation of the function at face vertexes on K_1, which is the first face of macro-element K indexed by the corner vertex $(x_{i_1,0}^{(1)}, \ldots, x_{i_n,0}^{(n)})$:

$$\frac{\partial^{l_1}}{\partial x_1^{l_1}} \frac{\partial^{\alpha_2}}{\partial x_2^{\alpha_2}} \cdots \frac{\partial^{\alpha_n}}{\partial x_n^{\alpha_n}} f(x_{i_1,0}^{(1)}, x_{i_n,l_2}^{(2)} \ldots, x_{i_n,l_n}^{(n)}),$$
$$0 \le l_1 \le k-1, \quad l_2, ..., l_n = 0, \text{ or } k.$$

The linear functional of taking nodal value at $(x_{i_1,0}^{(1)}, \ldots, x_{i_n,0}^{(n)})$, when restricted to the Hilbert space V_h with a weighted L^2 inner product on K_1, is represented by a Riesz vector $\psi^{(0,\alpha_2,\ldots,\alpha_n)}_{(x_{i_2,l_2}^{(2)},\ldots,x_{i_n,l_n}^{(n)}),K_1}$:

$$\int_{K_1} v(\mathbf{x}) \psi^{(0,\alpha_2,\ldots,\alpha_n)}_{(x_{i_2,l_2}^{(2)},\ldots,x_{i_n,l_n}^{(n)}),K_1}(\mathbf{x}) b^{(1)}(\mathbf{x}) d\mathbf{x} = v(x_{i_1,0}^{(1)}, x_{i_1,l_2}^{(2)} \ldots, x_{i_n,l_n}^{(n)}),$$

for all $v \in V_h$, where the weight is a bubble function defined by

$$b^{(1)}(\mathbf{x}) = \prod_{j=2}^{n} \prod_{l=0,k} (x_j - x_{i_j,l}^{(j)})^{k-1}. \tag{4.2}$$

The reason for introducing the bubble function as weight is to avoid boundary integrals when doing integration by parts in (4.3) below. Otherwise, if boundary integrals appear, one would require a higher regularity for the interpolated function f so that the traces of its higher order derivatives is L^1-integrable. These Riesz representation vectors form a dual basis whose action is to produce the L^2-projection, preserving C^{k-1}-Q_k (or its derivative spaces) polynomial v on the R^{n-1} face-square at the interpolation point; cf. [10, 23] for computing such a dual basis function. By using a macro-element whose derivative is no longer in the original piecewise polynomial space, we cannot use one set of dual basis as in Girault-Scott [8], as all derivatives of a polynomial there are still a polynomial of a lower degree.

Now, the D_α nodal derivative of a weak H^k function f is defined by

$$\frac{\partial^{l_1}}{\partial x_1^{l_1}}\frac{\partial^{\alpha_2}}{\partial x_2^{\alpha_2}}\cdots\frac{\partial^{\alpha_n}}{\partial x_n^{\alpha_n}} I_h f(x^{(1)}_{i_1,0}, x^{(2)}_{i_2,l_2},\dots,x^{(n)}_{i_n,l_2}) = (-1)^{|\alpha|-l_1}\int_K \frac{\partial^{l_1} f}{\partial x_1^{l_1}}(\mathbf{x}) \cdot \frac{\partial^{\alpha_2}}{\partial x_2^{\alpha_2}}\cdots\frac{\partial^{\alpha_n}}{\partial x_n^{\alpha_n}}\left[\psi^{(0,\alpha_2,\dots,\alpha_n)}_{(x^{(2)}_{i_2,l_2},\dots,x^{(n)}_{i_n,l_n}),K_1}(\mathbf{x}) b^{(1)}(\mathbf{x})\right] d\mathbf{x}. \tag{4.3}$$

Similarly, by rotating $x^{(1)}_{i_1,0}$ and $x^{(1)}_{i_j,0}$ and by rotating α_1 with another index α_j, we define all interpolation values on K. Globally, for each vertex $\mathbf{x}$ of $\mathcal{T}_h$, we choose a boundary square face in $K \in \mathcal{T}_h$ if $\mathbf{x} \in \partial\Omega$, otherwise a random R^{n-1} square face containing $\mathbf{x}$. The interpolation $I_h f$ is defined for the H^k function by the $I_h f$ nodal values as in (3.2). In particular, $I_h f$ preserves the homogeneous boundary conditions and preserves V_h functions,

$$I_h v = v \quad \forall v \in V_h.$$

Theorem 4.1. *Let $u \in H^r$ for some $r \geq k$, then*

$$\sum_{i=0}^{k} h^{i-k}|u - I_h u|_{H^i(\Omega)} \leq C h^{\min\{1,r-k\}}|u|_{H^r(\Omega)}, \tag{4.4}$$

where I_h is defined in (3.2) *with nodal values evaluated by* (4.3)*, interpolating u to the space V_h, defined in* (2.8)*.*

Proof. First, by (4.3), following the scaling argument of Scott-Zhang [19] or Girault-Scott [8] on the dual basis functions, one can show the stability of I_h:

$$|I_h u|_{H^r(\Omega)} \leq C|u|_{H^r(\Omega)}.$$

Next, by (3.4), I_h preserve C^{k-1}-Q_k polynomials locally, i.e., $I_h u = u$ if $u \in Q_k(S_K)$ where S_K is the union of all macro-elements touching K. Thus, by existence of local optimal-approximation polynomials, it is standard to show (4.4); cf. [19] for details. □

We apply the C^{k-1}-Q_k element to solve the following k-harmonic equations:

$$(-1)^k \Delta^k u = g, \quad \text{in } \Omega \subset R^n, \tag{4.5}$$

$$u = \cdots = \frac{\partial^{k-1}}{\partial \mathbf{n}^{k-1}} u = 0, \quad \text{on } \partial\Omega. \tag{4.6}$$

The finite element problem in the weak variational form for (4.5) is: find $u_h \in V_h$ such that

$$\int_\Omega \nabla^k u_h \nabla^k v_h = \int_\Omega g v_h \quad \forall v_h \in V_h. \tag{4.7}$$

Theorem 4.2. *Let u solve* (4.5) *and $u_h \in V_h$ solve* (4.7)*. Assume that $u \in H^r$ for some $r > k$, then*

$$|u - u_h|_{H^k(\Omega)} \leq C h^{\min\{1,r-k\}}|u|_{H^r(\Omega)}. \tag{4.8}$$

In addition, assume the solution of the dual problem has the regularity H^r. Then,

$$|u - u_h|_{H^m(\Omega)} \leq C h^{\min\{2,2(r-k)\}}|u|_{H^r(\Omega)}, \quad m = 0,\dots,k-1. \tag{4.9}$$

Remark 4.1. An H^r $(r > k)$ regularity is assumed for (4.9). For smooth domains, the regularity H^{k+s} can be proved for $g \in H^{s-k}(\Omega)$ and for any $s > 0$, in any dimension; see for instance, [7] and the references therein. A regularity of H^{k+s} with $s \in (0, 1/2)$ is obtained for n-dimensional k-harmonic equations on Lipschitz domains in [3, Theorem 1]. In a highly-referenced work [13], is shown an $H^{k+1/2}$ regularity for the n-dimensional Laplace operator on Lipschitz domains. For biharmonic equations, an $H^{k+1/2}$ regularity is also obtained on n-D Lipschitz domains in [1]. Some special regularity results on 3D polyhedral domains can also be found in [6, 7].

Proof of Theorem 4.2. As $V_h \subset H^k$ by Theorem 3.1, u_h is the Galerkin projection of u in the subspace. By Céa lemma, and (4.4),

$$|u - u_h|_{H^k} = \inf_{v_h \in V_h} |u - v_h|_{H^k} \le C h^{\min\{1, r-k\}} |u|_{H^r(\Omega)}.$$

For one lower order normal estimate, we use the standard duality argument to obtain

$$\begin{aligned} |u - u_h|^2_{H^{k-1}} &\le C h^{\min\{1, r-k\}} |w|_{H^r} |u - u_h|_{H^k} \\ &\le C |u - u_h|_{H^{k-1}} h^{\min\{2, 2(r-k)\}} |u|_{H^r(\Omega)}, \end{aligned} \tag{4.10}$$

where w is the solution of (4.7) with $g = u - u_h$. For the error bound (4.9) in further lower order norms, we use Poincaré inequality so that, for $u, u_h \in H^k(\Omega) \cap H_0^{k-1}(\Omega)$,

$$|u - u_h|_{H^m} \le C |u - u_h|_{H^{k-1}}, \quad 0 \le m \le k - 1.$$

We note that the error bound (4.9) for $m < k - 1$ is no longer of optimal order, i.e., is of a higher order than that of the interpolated error, $|u - I_h u|_{H^m}$. But the estimate is sharp, confirmed by the numerical test, in the next section. This can be shown following a trick of [12]. That is, (4.9) can be shown as a lower bound. ☐

5. Numerical tests

We compute four examples.

5.1. **Example 1.** In the first example, we solve (4.5) with $k = 2$, $n = 2$, and the exact solution

$$u = 2^{14} x^3 (1 - x)^2 y^4 (1 - y)^2. \tag{5.1}$$

So we use the C^1-Q_2 finite element. The initial grid is one square which is refined into 4 subsquares as the macro-element. Then we use the nested refinement to get higher level grids. The errors on various level grids and the orders of convergence are listed in Table 1. The finite element equation is solved by the conjugate gradient method, and the number of iterations are listed also in Table 1. The orders of convergence in H^1 and H^2 norm are truly optimal, as proved by Theorem 4.2.

5.2. **Example 2.** In the second example, we solve the triharmonic equation (4.5) where $n = 2$ and $k = 3$, i.e.,

$$-\Delta^3 u = g.$$

The exact solution is

$$u(x, y) = e^{\pi y} \sin(\pi x), \tag{5.2}$$

which provides nonhomogeneous boundary conditions in (4.6). The exact solution

TABLE 1. The errors $e_h = I_h u - u_h$ and orders $O(h^r)$ of convergence by the 2D C^1-Q_2 element for (5.1), Example 1.

grid	$\|e_h\|_{L^2}$	h^r	$\|e_h\|_{H^1}$	h^r	$\|e_h\|_{H^2}$	h^r	#CG
2	0.69506	0.0	3.90929	0.0	33.7811	0.0	7
3	0.42990	0.7	3.03623	0.4	42.9961	0.0	40
4	0.12061	1.8	0.89970	1.8	24.9250	0.8	139
5	0.03088	2.0	0.23386	1.9	12.9061	0.9	430
6	0.00776	2.0	0.05902	2.0	6.5088	1.0	1514
7	0.00194	2.0	0.01479	2.0	3.2614	1.0	5869

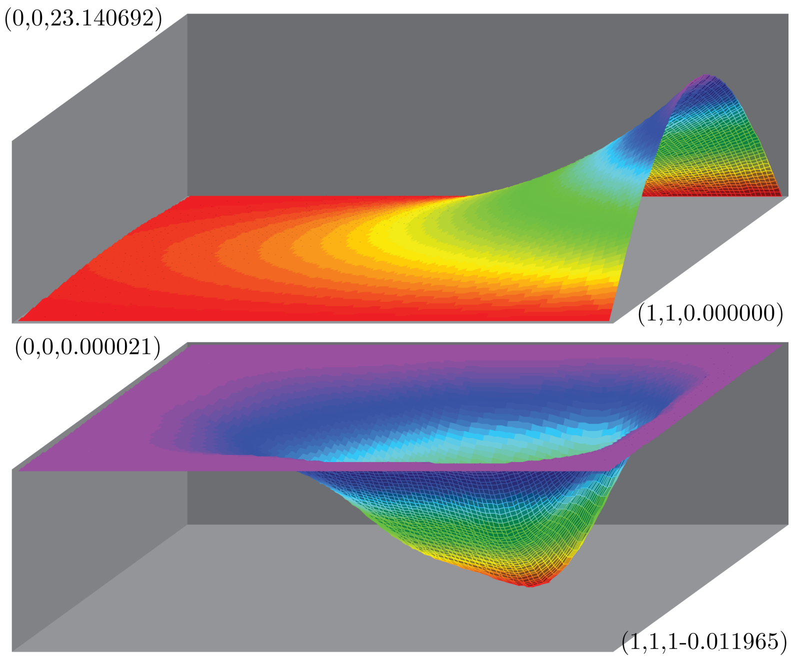

FIGURE 3. u and $(u - u_h)$ for (5.2) at level 3.

is plotted in Figure 3. We apply the 2D C^2-Q_3 finite element to solve the problem. The errors in various norms and the orders of convergence are listed in Table 2. The method does converge with the optimal order h in H^3 norm, as shown in Theorem 4.2, and also h^2 in H^2 norm.

5.3. **Example 3.** In this example, we solve the triharmonic equation

$$-\Delta^3 u = 0$$

on the L-shaped domain shown in Figure 4, with Dirichlet boundary conditions (4.6) given by the exact solution

$$u(x, y) = r^{2.5} \sin 2.5\theta, \tag{5.3}$$

TABLE 2. The errors $e_h = I_h u - u_h$ and orders $O(h^r)$ of convergence by the 2D C^2-Q_3 element for (5.2), Example 2.

grid	$\|e_h\|_{L^2}$	h^r	$|e_h|_{H^1}$	h^r	$|e_h|_{H^2}$	h^r	$|e_h|_{H^3}$	h^r
2	0.01131	0.0	0.0802	0.0	0.8029	0.0	10.679	0.0
3	0.00382	1.6	0.0241	1.7	0.2894	1.5	6.585	0.7
4	0.00099	1.9	0.0058	2.0	0.0796	1.9	3.509	0.9
5	0.00025	2.0	0.0014	2.0	0.0206	1.9	1.821	0.9
6	0.00006	2.0	0.0003	2.0	0.0052	2.0	0.931	1.0

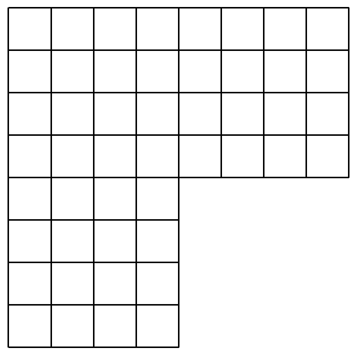

FIGURE 4. The level 3 grid for the L-shape domain in Example 3, for (5.3).

TABLE 3. The errors $e_h = I_h u - u_h$ and orders $O(h^r)$ of convergence by the 2D C^2-Q_3 element for singular solution (5.3), Example 3.

grid	$\|e_h\|_{L^2}$	h^r	$|e_h|_{H^1}$	h^r	$|e_h|_{H^2}$	h^r	$|e_h|_{H^3}$	h^r
2	0.0036	0.0	0.02377	0.0	0.2048	0.0	2.523	0.0
3	0.0018	1.0	0.01057	1.2	0.0983	1.1	1.896	0.4
4	0.0009	0.9	0.00510	1.1	0.0459	1.1	1.374	0.5
5	0.0004	1.0	0.00247	1.0	0.0214	1.1	0.983	0.5
6	0.0002	1.0	0.00119	1.1	0.0100	1.1	0.698	0.5

where (r, θ) are polar coordinates. We apply the 2D C^2-Q_3 finite element to solve the problem. Due to a singularity at the origin, we can see a large error near it, in Figure 5. But the error pollutes further away in the triharmonic equation, comparing to that of harmonic and biharmonic equations. The errors in various norms and the orders of convergence are listed in Table 3. The method does converge with the optimal order $h^{1/2}$ in H^3 norm, under the singularity. As the regularity index in (4.10) is $k + 1/2$ instead of $k + 1$, the order of convergence in lower norms is $2(1/2) = 1$ instead of 2, verified by the numerical data in Table 3.

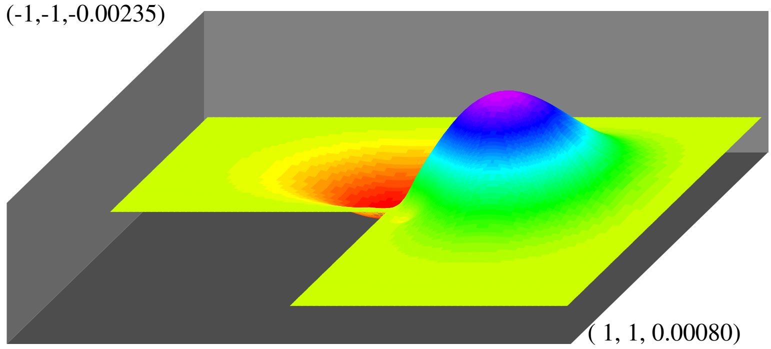

FIGURE 5. The error for the singular solution (5.3) on the level-4 grid in Example 3.

5.4. **Example 4.** In this example, we solve the triharmonic equation

$$-\Delta^3 u = 0$$

on the L-shaped domain with Dirichlet boundary conditions (4.6) given by the exact solution

$$u(x, y) = x^6 - y^6. \tag{5.4}$$

We apply the 2D C^2-Q_3 finite element on uniform grids on graded grids; see Figure 6. This is because a large error occurs at the boundary. The solution, the error on a uniform grid, and the error on a graded grid are plotted in Figure 7. The errors in various norms and the orders of convergence are listed in Table 4, on both family of grids.

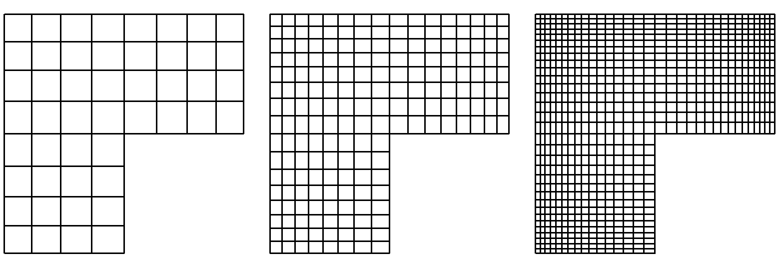

FIGURE 6. The level 3, level 4 and level 5 graded grids for problem (5.4) in Example 4.

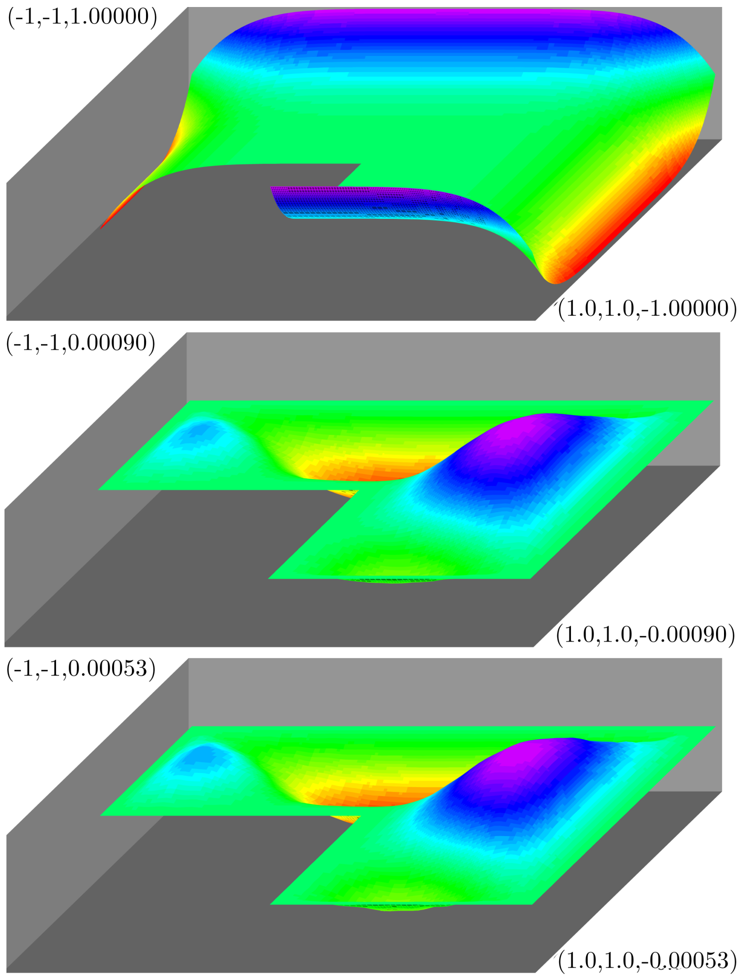

FIGURE 7. The solution (top) for (5.4), the error on the 4-th level uniform grid, and the error on the 4-th level graded grid (see Figure 6), in Example 4. The error on the graded grid is about 1/2 of that on the uniform grid.

Table 4. The errors $e_h = I_h u - u_h$ and orders $O(h^r)$ of convergence by the 2D C^2-Q_3 element for solution (5.4), Example 4.

grid	$\|e_h\|_{L^2}$	h^r	$|e_h|_{H^1}$	h^r	$|e_h|_{H^2}$	h^r	$|e_h|_{H^3}$	h^r
	On uniform grids, cf. Figure 4.							
2	0.008674	0.0	0.0496	0.0	0.4058	0.0	4.762	0.0
3	0.002472	1.8	0.0137	1.9	0.1377	1.6	2.834	0.7
4	0.000634	2.0	0.0034	2.0	0.0384	1.8	1.553	0.9
5	0.000116	2.5	0.0006	2.4	0.0092	2.1	0.808	0.9
	On graded grids, cf. Figure 6.							
2	0.008185	0.0	0.0475	0.0	0.3971	0.0	4.750	0.0
3	0.001974	2.1	0.0110	2.1	0.1194	1.7	2.731	0.8
4	0.000381	2.4	0.0020	2.4	0.0271	2.1	1.382	1.0
5	0.000093	2.0	0.0005	2.0	0.0061	2.1	0.639	1.1

References

[1] Vilhelm Adolfsson and Jill Pipher, *The inhomogeneous Dirichlet problem for Δ^2 in Lipschitz domains*, J. Funct. Anal. **159** (1998), no. 1, 137–190, DOI 10.1006/jfan.1998.3300. MR1654182 (99m:35048)

[2] Peter Alfeld and Maritza Sirvent, *The structure of multivariate superspline spaces of high degree*, Math. Comp. **57** (1991), no. 195, 299–308, DOI 10.2307/2938675. MR1079007 (92m:65017)

[3] M. S. Agranovich, *On the theory of Dirichlet and Neumann problems for linear strongly elliptic systems with Lipschitz domains* (Russian, with Russian summary), Funktsional. Anal. i Prilozhen. **41** (2007), no. 4, 1–21, 96, DOI 10.1007/s10688-007-0023-x; English transl., Funct. Anal. Appl. **41** (2007), no. 4, 247–263. MR2411602 (2009b:35070)

[4] J. H. Argyris, I. Fried, D. W. Scharpf, The TUBA family of plate elements for the matrix displacement method, The Aeronautical Journal of the Royal Aeronautical Society **72** (1968), pp. 514–517.

[5] Philippe G. Ciarlet, *The Finite Element Method for Elliptic Problems,* North-Holland Publishing Co., Amsterdam, 1978, Studies in Mathematics and its Applications, Vol. 4. MR0520174 (58 #25001)

[6] Monique Dauge, *Problèmes de Neumann et de Dirichlet sur un polyèdre dans $\mathbf{R}^3$: régularité dans des espaces de Sobolev L_p* (French, with English summary), C. R. Acad. Sci. Paris Sér. I Math. **307** (1988), no. 1, 27–32. MR954085 (90a:35057)

[7] Monique Dauge, *Elliptic Boundary Value Problems on Corner Domains*, Lecture Notes in Mathematics, vol. 1341, Springer-Verlag, Berlin, 1988. Smoothness and asymptotics of solutions. MR961439 (91a:35078)

[8] V. Girault and L. R. Scott, *Hermite interpolation of nonsmooth functions preserving boundary conditions*, Math. Comp. **71** (2002), no. 239, 1043–1074 (electronic), DOI 10.1090/S0025-5718-02-01446-1. MR1898745 (2003e:65012)

[9] J. Hu, Y. Q. Huang and Q. Lin. *The lower bounds for eigenvalues of elliptic operators-by nonconforming finite element methods.* arXiv:1112.1145v2[math.NA], 2013.

[10] Jun Hu, Yunqing Huang, and Shangyou Zhang, *The lowest order differentiable finite element on rectangular grids*, SIAM J. Numer. Anal. **49** (2011), no. 4, 1350–1368, DOI 10.1137/100806497. MR2817542 (2012h:65274)

[11] Jun Hu and Zhong-ci Shi, *Constrained quadrilateral nonconforming rotated $\mathcal{Q}_1$ element*, J. Comput. Math. **23** (2005), no. 6, 561–586. MR2190317 (2006k:65324)

[12] Jun Hu and Zhong-Ci Shi, *The best L^2 norm error estimate of lower order finite element methods for the fourth order problem*, J. Comput. Math. **30** (2012), no. 5, 449–460, DOI 10.4208/jcm.1203-m3855. MR2988473

[13] David Jerison and Carlos E. Kenig, *The inhomogeneous Dirichlet problem in Lipschitz domains*, J. Funct. Anal. **130** (1995), no. 1, 161–219, DOI 10.1006/jfan.1995.1067. MR1331981 (96b:35042)

[14] Vladimir Kozlov and Vladimir Maz′ya, *Asymptotic formula for solutions to elliptic equations near the Lipschitz boundary*, Ann. Mat. Pura Appl. (4) **184** (2005), no. 2, 185–213, DOI 10.1007/s10231-004-0108-6. MR2149092 (2006b:35070)

[15] Heejeong Lee and Dongwoo Sheen, *A new quadratic nonconforming finite element on rectangles*, Numer. Methods Partial Differential Equations **22** (2006), no. 4, 954–970, DOI 10.1002/num.20131. MR2230281 (2007a:65201)

[16] Chunjae Park and Dongwoo Sheen, *P_1-nonconforming quadrilateral finite element methods for second-order elliptic problems*, SIAM J. Numer. Anal. **41** (2003), no. 2, 624–640 (electronic), DOI 10.1137/S0036142902404923. MR2004191 (2004i:65125)

[17] M. J. D. Powell and M. A. Sabin, *Piecewise quadratic approximations on triangles*, ACM Trans. Math. Software **3** (1977), no. 4, 316–325. MR0483304 (58 #3319)

[18] Larry L. Schumaker, *Spline Functions: Basic Theory*, 3rd ed., Cambridge Mathematical Library, Cambridge University Press, Cambridge, 2007. MR2348176 (2008i:41002)

[19] L. Ridgway Scott and Shangyou Zhang, *Finite element interpolation of nonsmooth functions satisfying boundary conditions*, Math. Comp. **54** (1990), no. 190, 483–493, DOI 10.2307/2008497. MR1011446 (90j:65021)

[20] Chung Tze Shih, *On a spline finite element method* (Chinese, with English summary), Math. Numer. Sinica **1** (1979), no. 1, 50–72. MR656879 (83e:73059)

[21] Ming Wang and Jinchao Xu, *Minimal finite element spaces for $2m$-th-order partial differential equations in R^n*, Math. Comp. **82** (2013), no. 281, 25–43, DOI 10.1090/S0025-5718-2012-02611-1. MR2983014

[22] Ming Wang, Zhong-Ci Shi, and Jinchao Xu, *Some n-rectangle nonconforming elements for fourth order elliptic equations*, J. Comput. Math. **25** (2007), no. 4, 408–420. MR2337403 (2008e:65366)

[23] Xuejun Xu and Shangyou Zhang, *A new divergence-free interpolation operator with applications to the Darcy-Stokes-Brinkman equations*, SIAM J. Sci. Comput. **32** (2010), no. 2, 855–874, DOI 10.1137/090751049. MR2609343 (2011g:76108)

[24] Shangyou Zhang, *A family of 3D continuously differentiable finite elements on tetrahedral grids*, Appl. Numer. Math. **59** (2009), no. 1, 219–233, DOI 10.1016/j.apnum.2008.02.002. MR2474112 (2010a:65250)

[25] Shangyou Zhang, *On the full C_1-Q_k finite element spaces on rectangles and cuboids*, Adv. Appl. Math. Mech. **2** (2010), no. 6, 701–721. MR2719052 (2011i:65230)

LMAM and School of Mathematical Sciences, Peking University, Beijing 100871, People's Republic of China

E-mail address: hujun@math.pku.edu.cn

Department of Mathematical Sciences, University of Delaware, Newark, Delawre 19716

E-mail address: szhang@udel.edu